Frontiers in Heat and Mass Transfer (FHMT), 20, 5 (2023)
DOI: 10.5098/hmt.20.5

Global Digital Central
ISSN: 2151-8629

Frontiers in Heat and Mass Transfer

Available at www.ThermalFluidsCentral.org

FINITE ELEMENT ANALYSYS OF RADIATIVE UNSTEADY MHD VISCOUS DISSIPATIVE MIXED CONVECTION FLUID FLOW PAST AN IMPULSIVELY STARTED OSCILLATING PLATE IN THE PRESENCE OF HEAT SOURCE

D. Santhi Kumari[a,*], Venkata Subrahmanyam Sajja[a], P. M. Kishore[b,†]

[a]* *Research Scholar, Department of Engineering Mathematics, Koneru Lakshmaiah Education Foundation, Guntur, A.P., India.*
[a] *Department of Engineering Mathematics, Koneru Lakshmaiah Education Foundation, Guntur, A.P., India.*
[b] *Department of Mathematics, Geethanjali Institute of Science and Technology, Nellore, A.P., India.*

ABSTRACT

The aim of present study is an influence of viscous dissipation and heat source on an unsteady MHD mixed convective, fluid flow past an impulsively started oscillating plate embedded in a porous medium in presence of magnetic field, heat and mass transfer. The modeling equations are converted to dimensionless equations then solved through Galerkin finite element method and discussed in the flow distributions with the help of MATLAB. Numerical results for the velocity, temperature and concentration distributions as well as the skin-friction coefficient, Nusselt number and Sherwood number are discussed in detail and displayed graphically for various physical parameters. It is observed that increasing the values of porous medium improves the velocity profile, while increasing 'M' and Prandtl number decreases it. As the values of the heat source parameter increase, the temperature profile decreases. This model may be useful in view of lab experimental results for correctness and applicability and useful to analyze the fluid behavior in thermal engineering industries with the influence of the thermal, magnetic and chemical reaction effects etc. A comparison of present results with previously published results shows an excellent agreement.

Keywords: *Magnetic field, Porous medium, viscous dissipation, Hall current, Heat Source*

1. INTRODUCTION

Current research has been mingled with a mixed convective flow of porous media. The mathematical developments were used to characterize the flow within porous media prior to 1969 reviewed. Flow in porous media is important in many areas of science and technology including biology, soil science, reaction engineering, waste treatment, and separation science. The mixed physical process of MHD convection flow has been gaining increasing research attention owing to its increased utilization in diverse physical chemical and engineering applications.

In the presence of strong magnetic fields, the Hall Effect becomes an important mechanism for electrical conduction in ionized gases and plasmas. Unlike metals, the number density of charge carriers in ionized gases is low, which results in anisotropic behavior of the electrical properties. Hence, a current is induced in the direction normal to both the electric and magnetic fields. The Hall Effect has important engineering applications, such as the Hall generators, Hall probes, and Hall Effect thrusters used for space missions.

The study of heat and mass transfer with chemical reactions is of great practical importance to engineers and scientists because of its almost universal occurrence in many branches of science and engineering. Combined heat and mass transfer in fluid-saturated porous media finds applications in a variety of engineering processes such as heat exchanger devices, petroleum reservoirs, chemical catalytic reactors and processes, geothermal and geophysical engineering, moisture migration in a fibrous insulation and nuclear waste disposal and others.

As of late, magneto hydrodynamics boundary layer stream and heat transfer of electrically conducting liquids have different science, designing, and mechanical applications such as petrol businesses, precious stone development, geothermal designing, atomic reactors, fluid metals, streamlined features, and metallurgical cycles. MHD principles also find its applications in Medicine and Biology.

Hydro magnetic unsteady mixed convection and mass transfer past a vertical porous plate were investigated by Sharma and Chaudhary (2008). The effects of thermal radiation and viscous dissipation on MHD heat and mass diffusion flow past an oscillating vertical plate embedded in a porous medium with variable surface conditions is described by Kishore et al. (2012). Finite element analysis of soret and radiation effects on transient MHD free convection from an impulsively started infinite vertical plate with heat absorption is narrated by Jithender Reddy et al. (2014). An attempt to study an unsteady oscillatory hydro magnetic mixed convection flow through a porous medium with periodic temperature variation by Ramana Reddy et al. (2014). Thermal diffusion and diffusion thermo effects on unsteady MHD fluid flow past a moving vertical plate embedded in porous medium in the presence of Hall current and rotating system is reported Jithender Reddy et al. (2016). Transfer effects on an unsteady MHD mixed convective flow past a vertical plate with chemical reaction is chronicled Srinivasa Raju (2017). Venkateshwara Raju et al. (2018)analyzed unsteady MHD free convection Jeffery fluid flow of radiating and reacting past a vertical

*Research Scholar .Presently at Department of Science & Humanities, Rise Krishna Sai Prakasam Group of Institutions, Ongole, Andhra Pradesh, India
†*Corresponding author.Email:subrahmanyam@kluniversity.in*.

Global Digital Central
ISSN: 2151-8629

porous plate in slip-flow regime with heat source. Chemical reaction and radiation effects on MHD free convection flow past an exponentially accelerated vertical porous plate is stated Sitamahalakshmi et al. (2019). Effects of thermal radiation on MHD chemically reactive flow past an oscillating vertical porous plate with variable surface conditions and viscous dissipation is expressed by Prabhakar Reddy et al. (2019). FDM and FEM correlative approach on unsteady heat and mass transfer flow through a porous medium is conveyed by Shankar Goud et al. (2020). Saddam Atteyia Mohammad (2020) is analyzed effects of variable viscosity on heat and mass transfer by MHD mixed convection flow along a vertical cylinder embedded in a non-darcy porous medium. Anil Kumar et al. (2020) described thermal radiation effect on MHD heat transfer natural convective nanofluid flow over an impulsively started vertical plate. Anil Kumar et al. (2021) investigated effects of Soret, Dufour, Hall current and rotation on MHD natural convective heat and mass transfer flow past an accelerated vertical plate through a porous medium. Mateo et al. (2020) studied unsteady MHD radiating and reacting mixed convection past an impulsively started oscillating plate.

Keeping in mind the work done by previous researchers, we attempted to analyze heat source and viscous dissipation effects on unsteady magneto hydrodynamic mixed convective heat and mass transfer flow of a fluid past an oscillating plate embedded in a porous medium in the presence of constant wall temperature and concentration. The novelty of this work is the consideration of heat source/sink and viscous dissipation in conservation of energy. We have extended the work of Matao et al. (2020) by including the presence of above-mentioned flow parameters. This is not a simple extension of the previous work. It varies several aspects from that such as the presence of mass transfer in the momentum equation, radiation absorption inclusion in the energy equation and the addition of species diffusion equation. Apart from the modification of set of governing equations, we also changed the method of solution due to the existence of nonlinear-coupled partial differential equations, which are solved, by Galerkin finite element method, with its computational cost efficiency, has been employed for obtaining the solutions. The consequent changes and comportment of diverse aspects such as the concentration, velocity, temperature, and engineering parameters have been comprehensively focused on observing the possible changes in the behavior of the fluid.

2. MATHEMATICAL ANALYSIS

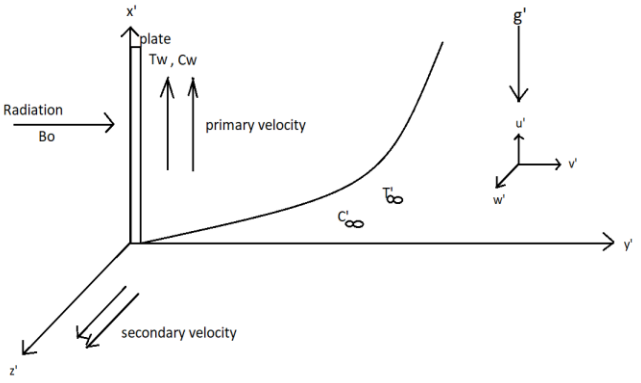

Fig. 1 Coordinate system and physical configuration

Consider the unsteady MHD flow of viscous incompressible electrically conducting, radiating and reacting fluid pastan impulsively started oscillating infinite vertical plate taking into an account viscous dissipation with variable temperature and constant mass diffusion presence of heat source. A uniform magnetic field $\vec{B}$ of strength B_0 is applied in the direction perpendicular to the fluid flow. In the Cartesian co-ordinate system, the x'-axis is taken along the plate in the vertically upward direction, the y'-axis perpendicular to the direction of the plate and the z'-axis is normal to the $x'y'$-plane. The physical model of the problem is shown in Fig.1. Initially, at time $t' \le 0$ the temperature of the fluid and the plate is $T'_\infty$and the concentration of the fluid is C'_∞. Subsequently, at time $t' > 0$, the plate starts oscillating in its own plane with frequency ω', the temperature of the plate and the concentration of the fluid, respectively are raised to T'_wandC'_w. It is assumed that the radiation heat flux in the x'- direction is negligible as compared to that in y'- direction. As the plate is of infinite extent and electrically non-conducting, all the physical quantities, except the pressure, are functions of $y'$and t'.

The generalized Ohm's law on taking Hall current into account Cowling (1957) is given by

$$\vec{J} + \frac{\omega_e \tau_e}{B_0}\left(\vec{J} \times \vec{B}\right) = \sigma\left(\vec{B} + \vec{q} \times \vec{B}\right) \tag{1}$$

Where $\vec{q}, \vec{B}, \vec{E}, \vec{J}, \sigma, \omega_e$and τ_e are respectively,velocity vector, magnetic field vector, electric field vector, current density vector, electric conductively, cyclotron frequency and electron collision time.

The equation of continuity $\nabla . \vec{q} = 0$ gives $v' = 0$ everywhere in the flow since there is no variation of the flow in y'– direction, where $\vec{q} = (u', v', w')$ and u', v', w' are respectively, velocity components along the coordinate axes.

The magnetic Reynolds number is so small that the induced magnetic field produced by the fluid motion is neglected. The solenoid relation $\nabla . \vec{B} = 0$ for the magnetic field $\vec{B} = (B_{x'}, B_{y'}, B_{z'})$ gives $B_{y'}$= constant sayB_0. i.e.,$\vec{B} = (0, B_0, 0)$everywhere in the flow. The conservation of electric current $\nabla . \vec{J} = 0$ yields $j_{y'} =$ constant, where$\vec{J} = (j_{x'}, j_{y'}, j_{z'})$. This constant is zero since $j_{y'} = 0$at the plate which is electrically non-conducting. Hence,$j_{y'} = 0$ everywhere in the flow. In view of the above assumption, Equation (1) yields

$$j_{x'} - m j_{y'} = \sigma(E_{x'} - w' B_0) \tag{2}$$

$$j_{z'} + m j_{x'} = \sigma(E_{z'} + u' B_0) \tag{3}$$

Where $m(= \omega_e \tau_e)$ is the Hall parameter which represents the ratio of electron-cyclotron frequency and the electron-atom collision frequency. Since the induced magnetic field is neglected, Maxwell equation $\nabla \times \vec{E} = \frac{\partial \vec{H}}{\partial t}$ becomes $\nabla \times \vec{E} = 0$ which gives $\frac{\partial E_{x'}}{\partial y'} = 0$ and $\frac{\partial E_{z'}}{\partial y'} = 0$. This implies that $E_{x'}$ =constant and$E_{z'} =$ constant everywhere in the flow and choose this constant equal to zero, i.e., $E_{x'} = E_{z'} = 0$. Solving for $j_{x'}$and$j_{z'}$ from Equations (2)and(3), on using $E_{x'} = E_{z'} = 0$,

$$j_{x'} = \frac{\sigma B_0}{1 + m^2}(m u' - w') \tag{4}$$

$$j_{z'} = \frac{\sigma B_0}{1 + m^2}(m w' + u') \tag{5}$$

Taking into consideration the assumptions made above, under the Boussinesq's approximation, and using Equations (4)and(5), the basic governing equations of the flow are derived as:

2.1 GOVERING EQUATIONS:

The description of the physical problem closely follows that of Rajput et al. (2016). This introduces unsteadiness in the flow field. The physical model and the coordinate system are shown Fig.1.

Global Digital Central
ISSN: 2151-8629

Continuity Equation:

$$\frac{\partial v'}{\partial y'} = 0 \tag{6}$$

Momentum Equation:

$$\frac{\partial u'}{\partial t'} = \nu \frac{\partial^2 u}{\partial y'^2} - \frac{\sigma B_o^2}{\rho\left(1+m^2\right)}\left(u' + mw'\right) - \frac{\nu u'}{K_1} \tag{7}$$

$$+ g\beta(T' - T_\infty') + g\beta^*(C' - C_\infty')$$

$$\frac{\partial w'}{\partial t'} = \nu \frac{\partial^2 w'}{\partial y'^2} + \frac{\sigma B_o^2}{\rho\left(1+m^2\right)}\left(mu' - w'\right) - \frac{\nu w'}{K_1} \tag{8}$$

Energy Equation:

$$\rho C_P \frac{\partial T'}{\partial t'} = k \frac{\partial^2 T'}{\partial y'^2} - \frac{\partial q_r}{\partial y'} + \mu\left(\frac{\partial u'}{\partial y'}\right)^2 - Q_0\left(T' - T_\infty'\right) \tag{9}$$

Concentration Equation:

$$\frac{\partial C'}{\partial t'} = D \frac{\partial^2 C'}{\partial y'^2} - \gamma_r'\left(C' - C_\infty'\right) \tag{10}$$

The initial and boundary conditions for the problem are:

$$t' \le 0;\ u' = 0,\ w' = 0,\ T' = T_\infty',\ C' = C_\infty' \qquad for\ \ all\ \ y' \ge 0$$

$$t' > 0;\ u' = u_0 \cos\omega' t',\ w' = 0,\ T' = T_\infty' + (T_w' - T_\infty')\frac{t' u_0^2}{\nu},\ C' = C_w' \ \ at\ y' = 0$$

$$u' \to 0,\ w' \to 0,\ T' \to T_\infty',\ C' \to C_\infty' \qquad as\ \ y' \to \infty \tag{11}$$

The radiation heat flux r q under the Roseland approximationMagyari and Pantokratoras (2011) expressed by

$$q_r = -\frac{4\sigma^*}{3k^*}\frac{\partial T'^4}{\partial y'} \tag{12}$$

Where σ^* is the Stefan-Boltzmann constant and k^* is the mean absorption coefficient. It is assumed that temperature difference within the flow are sufficiently small, then Equation (11) can be liberalized by expanding T'^4 into the Taylor series about T_∞' which, after neglecting higher-order terms, takes the form:

$$T'^4 \cong 4T_\infty'^3 T' - 3T_\infty'^4 \tag{13}$$

In view of Equations (11) and (12), Equation (8) reduces to

$$\rho C_P \frac{\partial T'}{\partial t'} = k\left(1 + \frac{16\sigma^* T_\infty'^3}{3kk^*}\right)\frac{\partial^2 T'}{\partial y'^2} + \mu\left(\frac{\partial u'}{\partial y'}\right)^2 - Q_0\left(T' - T_\infty'\right) \tag{14}$$

Using Equation (14) and introducing the non-dimensional quantities:

$$u = \frac{u'}{u_0}\ \ y = \frac{y' u_0}{\nu}\ \ t = \frac{t' u_0^2}{\nu}\ \ w = \frac{w'}{u_0}\ \ \omega = \frac{\omega' \nu}{u_0^2}\ \ S_c = \frac{\nu}{D}\ \ P_r = \frac{\mu C_p}{k}$$

$$M = \frac{\sigma \mu_0^2 H_0^2 \nu}{\rho v_0^2}\ \ K_r = \frac{\gamma' \nu}{u_0^2}\ \ R = \frac{16\sigma^* T_\infty'^3}{3k\,k^*}\ \ \theta = \frac{T' - T_\infty'}{T_w' - T_\infty'}$$

$$\phi = \frac{C' - C_\infty'}{C_w' - C_\infty'}\ \ G_m = \frac{g\beta\nu\left(C_w' - C_\infty'\right)}{u_0^3}\ \ G_r = \frac{\nu\, g\ \beta\left(T_w' - T_\infty'\right)}{u_0^3}$$

$$S = \frac{Q_0}{\rho\, C_P\, \upsilon}\ \ E_c = \frac{u_0^2}{C_P\left(T_w' - T_\infty'\right)}\ \ K = \frac{K_1 u_0^2}{\nu^2} \tag{15}$$

into Equations (6) (7) (9) and (13) the following are obtained in non-dimensional form as follows

$$\frac{\partial u}{\partial t} = \frac{\partial^2 u}{\partial y^2} - \left(\frac{M}{\left(1+m^2\right)}\right)(u + mw) - \frac{u}{K} + Gr\theta + Gm\phi \tag{16}$$

$$\frac{\partial w}{\partial t} = \frac{\partial^2 w}{\partial y^2} + \frac{M}{\left(1+m^2\right)}(mu - w) - \frac{w}{K} \tag{17}$$

$$\frac{\partial \theta}{\partial t} = \frac{(1+R)}{P_r}\frac{\partial^2 \theta}{\partial y^2} + E_c\left(\frac{\partial u}{\partial y}\right)^2 - S\theta \tag{18}$$

$$\frac{\partial \phi}{\partial t} = \frac{1}{S_c}\frac{\partial^2 \phi}{\partial y^2} - K_r \phi \tag{19}$$

The initial and boundary conditions Equation (10), in non-dimensional form become:

$$t \le 0;\ u = 0,\ w = 0,\ \theta = 0,\ \phi = 0 \qquad for\ \ all\ \ y \ge 0$$

$$t > 0;\ u = \cos\omega t,\ w = 0,\ \theta = t,\ \phi = 1 \qquad at\ \ y = 0$$

$$u \to 0,\ w \to 0,\ \theta \to 0,\ \phi \to 0 \qquad as\ \ y \to \infty \tag{20}$$

3. SOLUTION OF THE PROBLEM

The set of partial differential equations given (16)–(19) are highly non-linear therefore cannot be solved analytically. Thus, for the solution of this problem, Galerkin finite element method by Bathe (1996) and Reddy (1985) has been implemented. The finite element method is a powerful technique for solving differential or partial differential equations as well as for integral equations. This method is so general that it can be applied even for integral equations including heat transfer fluid mechanics, chemical processing, solid mechanics, electrical systems and other fields also. The steps involved in the finite element analysis are as in follows

For equation (16), taking the linear element over two nodded (e), $(y_j \le y \le y_k)$ is

$$\int_{y_j}^{y_k}\left\{N^T\left[\frac{\partial^2 u}{\partial y^2} - M^*(u + mw) - \frac{\partial u}{\partial t} - \frac{u}{K_1} + Gr\theta + Gm\phi\right]\right\}dy = 0 \tag{21}$$

In equation (21) integrating the first term using by parts method and neglecting that term. After that, replace Galerkin finite element approximation over the two hugged linear variable $'(e)'$ of the form , $u^{(e)} = N^{(e)}\zeta^{(e)}$,here$\zeta^{(e)} = [\zeta_j \zeta_k]$, , $\phi^{(e)} = [u_j\ u_k]^T$,$\zeta_j = \frac{y - y_j}{h}$, $\zeta_j = \frac{y_k - y}{h}$ $h = y_k - y_j$ are the basis functions along the j^{th} and k^{th} nodes , velocity components u_j , u_k . The consecutive element equations $y_{i-1} \le y \le y_i$ and $y_i \le y \le y_{i+1}$, adding the element equations by inter-element connectivity.

The following difference strategy obtained when putting the row corresponding to the node i to zero.

$$\frac{1}{6}\left[\dot{u}_{i-1} + 4\dot{u}_i + \dot{u}_{i+1}\right] + \frac{1}{h^2}\left[-u_{i-1} + 2u_i - u_{i+1}\right] + \frac{M^*}{6}\left[u_{i-1} + 4u_i + u_{i+1}\right] = P \tag{22}$$

The following system of equations is got after applying Crank-Nicholson method on (16)

$$A_1 u_{i-1}^{n+1} + A_2 u_i^{n+1} + A_3 u_{i+1}^{n+1} = A_4 u_{i-1}^n + A_5 u_i^n + A_6 u_{i+1}^n + 6Pk \tag{23}$$

$$B_1 w_{i-1}^{n+1} + B_2 w_i^{n+1} + B_3 w_{i+1}^{n+1} = B_4 w_{i-1}^n + B_5 w_i^n + B_6 w_{i+1}^n + 6kM^* \tag{24}$$

$$C_1\theta_{i-1}^{n+1} + C_2\theta_i^{n+1} + C_3\theta_{i+1}^{n+1} = C_4\theta_{i-1}^n + C_5\theta_i^n + C_6\theta_{i+1}^n + 6kQP^* \tag{25}$$

$$D_1\phi_{i-1}^{n+1} + D_2\phi_i^{n+1} + D_3\phi_{i+1}^{n+1} = D_4\phi_{i-1}^n + D_5\phi_i^n + D_6\phi_{i+1}^n \tag{26}$$

Where

DOI: 10.5098/hmt.20.5 ISSN: 2151-8629

$$A_1 = -3r+1+\left(M^*+\frac{1}{K}\right)\frac{1}{2}rh^2,\ A_2 = 6r+4+\left(M^*+\frac{1}{K}\right)2rh^2,$$
$$A_3 = -3r+1+\left(M^*+\frac{1}{K}\right)\frac{1}{2}rh^2,\ A_4 = 3r+1-\left(M^*+\frac{1}{K}\right)\frac{1}{2}rh^2,$$
$$A_5 = -6r+4-\left(M^*+\frac{1}{K}\right)2rh^2,\ A_6 = 3r+1-\left(M^*+\frac{1}{K}\right)\frac{1}{2}rh^2 \quad (27)$$

$$B_1 = -3r+1+\left(M^*+\frac{1}{K}\right)\frac{1}{2}rh^2,\ B_2 = 6r+4+\left(M^*+\frac{1}{K}\right)2rh^2$$
$$B_3 = -3r+1+\left(M^*+\frac{1}{K}\right)\frac{1}{2}rh^2,\ B_4 = 3r+1-\left(M^*+\frac{1}{K}\right)\frac{1}{2}rh^2 \quad (28)$$
$$B_5 = -6r+4-\left(M^*+\frac{1}{K}\right)2rh^2,\quad B_6 = 3r+1-\left(M^*+\frac{1}{K}\right)\frac{1}{2}rh^2$$

$$C_1 = -3r+P^*+\frac{1}{2}P^*Srh^2,\ C_2 = 6r+4P^*+2P^*Srh^2$$
$$C_3 = -3r+P^*+\frac{1}{2}P^*Srh^2,\ C_4 = 3r+P^*-\frac{1}{2}P^*Srh^2 \quad (29)$$
$$C_5 = -6r+4P^*-2P^*Srh^2,\ C_6 = 3r+P^*-\frac{1}{2}P^*Srh^2$$

$$D_1 = -3r+S_c+\frac{1}{2}K_r\,S_crh^2,\ D_2 = 6r+4S_c+2K_rS_crh^2$$
$$D_3 = -3r+S_c+\frac{1}{2}K_rS_crh^2,\ D_4 = 3r+S_c-\frac{1}{2}K_r\,S_crh^2 \quad (30)$$
$$D_5 = -6r+4S_c-2K_r\,S_crh^2,\ D_6 = 3r+S_c-\frac{1}{2}K_r\,S_crh^2$$

$$Q = E_c\left(\frac{\partial u}{\partial y}\right)^2,\ M^* = \frac{M}{\left(1+m^2\right)},\ P = (G_r)\theta+(G_m)\phi-M^*mw$$

$$P^* = \frac{P_r}{1+R},\ r = \frac{k}{h^2}$$

Here Index i designates to space and j for time. Theequations at every internal nodal point on a particular n-level constitute a tri-diagonal system of equations. They are solved by making use of the Thomas algorithm. A grid independent test is employed to get the solution with the least error. It is carried out by testing with various grid sizes.The equations at each internal nodal point on a particular n-level represent a tri-diagonal system of equations. So, in the equations (27) to (30), taking i = 1(1) and using the boundary conditions (20), the following tri-diagonal system of equations are obtained. The tri-diagonal system is solved by making use of Thomas algorithm for which a numerical code is executed using MATLAB Program. To prove the convergence of the numerical scheme, the computation is carried out for small changed values of h and k and the iterations performed until a tolerance 10−8 is achieved. No notable change is observed in the values of $u,\ w,\ \theta and\ \phi$. Thus, the Galerkin finite element method is convergent and stable.

The dimensionless primary and secondary skin frictions are given by

$\tau_x = \frac{\partial u}{\partial y}$ at y = 0 and $\tau_z = \frac{\partial w}{\partial y}$ at y = 0.

The dimensionless Nusselt and Sherwood numbers are given by

$Nu = \frac{\partial \theta}{\partial y}$ at y = 0 and $S_h = \frac{\partial \phi}{\partial y}$ at y = 0.

From table 1 it is clear that skin friction decreases due to an increase in Hartmann number. it is noticed that the skin friction increases due to an increase in porous medium.

From the table 2 it is clear that N_u increases with the increasing values of P_r, S and decreases with the increasing values of R, E_c.

From the table 3 it is clear that S_h increases with increasing values of S_c and decreases due to an increase in K_r, t.

4. RESULT AND DISCUSSIONS

The parameters like $M, R, m, K, G_r, G_m, P_r, S, E_c, S_c, K_r$ are shown in graphs.

$$Kr = 0.2, Gr = 10, Gm = 10, M = 2,$$
$$m = 0.5, R = 2, t = 2, Pr = 7, Sc = 2.01,$$
$$S = 2, K = 0.5, Ec = 0.1$$

Table 1: Numerical values of Primary and Secondary Skin Frictions

Gr	Gm	M	m	K		ωt Degrees	R	Pr	Ec	S	Sc	Kr	t	τ_x	τ_z
10	10	1	0.5	1		30	1	0.71	0.001	10	0.22	0.5	0.2	-2.013825	-0.131652
20	10	1	0.5	1		30	1	0.71	0.001	10	0.22	0.5	0.2	-2.366952	-0.134717
10	20	1	0.5	1		30	1	0.71	0.001	10	0.22	0.5	0.2	-5.141829	-0.182711
10	10	2	0.5	1		30	1	0.71	0.001	10	0.22	0.5	0.2	-1.752037	-0.248861
10	10	1	1	1		30	1	0.71	0.001	10	0.22	0.5	0.2	-2.112821	-0.168109
10	10	1	0.5	2		30	1	0.71	0.001	10	0.22	0.5	0.2	-2.181828	-0.136459
10	10	1	0.5	1		45	1	0.71	0.001	10	0.62	0.5	0.2	-2.283051	-0.117425

Table 2. Numerical values of Nusselt number

P_r	R	E_c	S	t	N_u
0.71	1	0.001	10	0.2	0.470071
7.00	1	0.001	10	0.2	1.480354
0.71	2	0.001	10	0.2	0.383755
0.71	1	0.002	10	0.2	0.469959
0.71	1	0.001	15	0.2	0.538483
0.71	1	0.001	10	0.3	0.659245

Table 3. Numerical values of Sherwood number

S_c	K_r	t	S_h
0.22	0.5	0.2	0.651024
0.62	0.5	0.2	1.093765
0.22	1.0	0.2	0.707223
0.22	0.5	0.3	0.554695

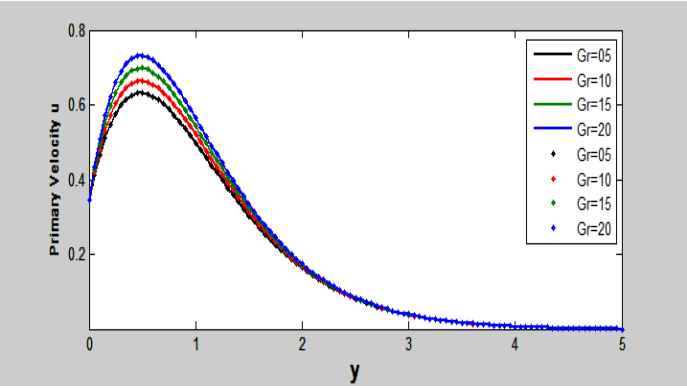

Figure 2: Primary velocity distribution with respect to G_r .

Figure 2 depict the comparison of the present work's velocity profile with the previous study done by Mateo et al. (2020). For fluid velocity, this figure shows excellent agreement (under some limiting conditions) between the current work and previously published work Mateo et al. (2020).

It is seen from **figure-3** that the primary velocity falls when M increases. That is the primary fluid motion is retarded due to application of transverse magnetic field. This phenomenon clearly agrees with the fact that Lorentz force that appears due to interaction of the magnetic field and fluid velocity resists the fluid motion.

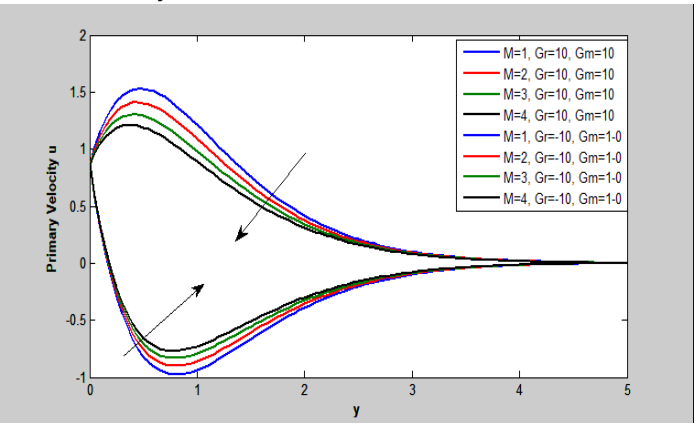

Figure 3: Primary velocity for varying M .

It can be observed from the figure 5 that G_r signifies the relative effect of the thermal buoyancy force to the viscous hydrodynamic force in the boundary layer. As expected, it is observed that there was a rise in the velocity due to the enhancement of thermal buoyancy force. Also, as G_r increases, the peak values of the velocity increase rapidly near the porous plate and then decays smoothly to the free stream velocity.

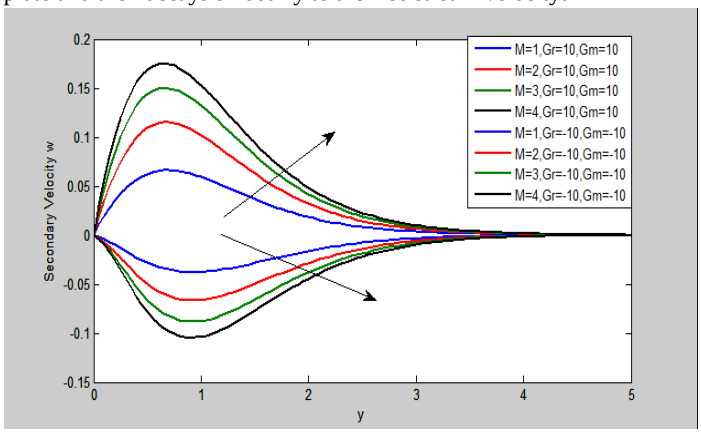

Figure 4: Secondary velocity for varying M .

The secondary velocity increases with increasing M , because of less kinetic viscosity.

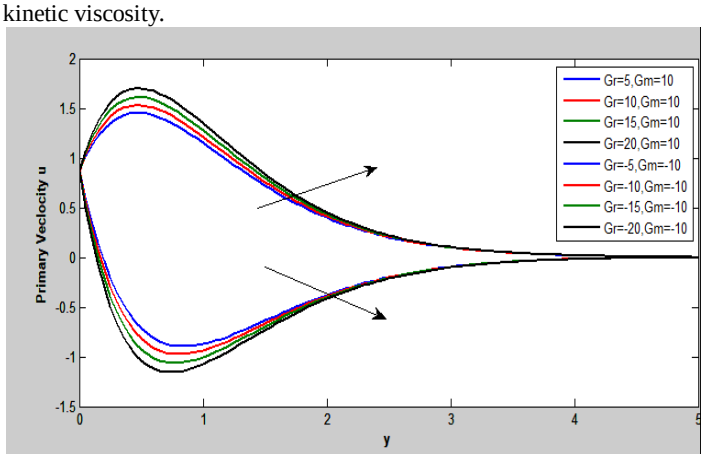

Figure 5: Primary velocity for varying G_r .

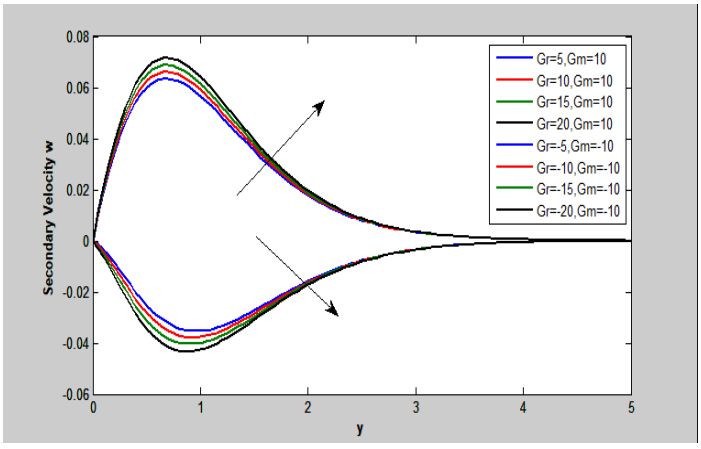

Figure 6: Secondary velocity distribution with respect to G_r .

G_r signifies the relative effect of the thermal buoyancy force to the viscous hydrodynamic force in the boundary layer. As expected, it is observed that there was a rise in the velocity due to the enhancement of thermal buoyancy force. Also, as G_r increases, the peak values of the

velocity increase rapidly near the porous plate and then decays smoothly to the free stream velocity.

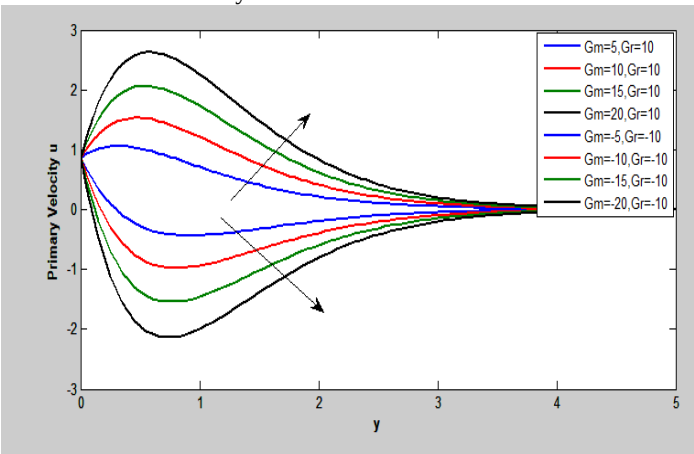

Figure 7: Primary velocity for varying G_m.

G_m defines the ratio of the species buoyancy force to the viscous hydrodynamic force. As expected, the fluid velocity increases and the peak value is more distinctive due to increase in the species buoyancy force. The velocity distribution attains a distinctive maximum value in the vicinity of the plate and then decreases properly to approach the free stream value. It is noticed that the velocity increases with increasing values of G_m.

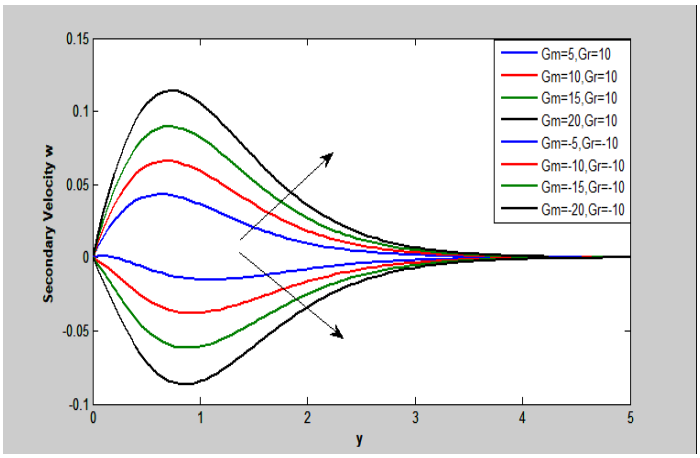

Figure 8: Secondary velocity distribution with respect to G_m.

G_m defines the ratio of the species buoyancy force to the viscous hydrodynamic force. As expected, the fluid velocity increases and the peak value is more distinctive due to increase in the species buoyancy force. The velocity distribution attains a distinctive maximum value in the vicinity of the plate and then decreases properly to approach the free stream value. It is noticed that the velocity increases with increasing values of G_m.

From Figure 9 that primary velocity is increased due to increase in K. Physically, increase in K tends to decrease the resistance of the porous medium as a result increase the fluid velocity.

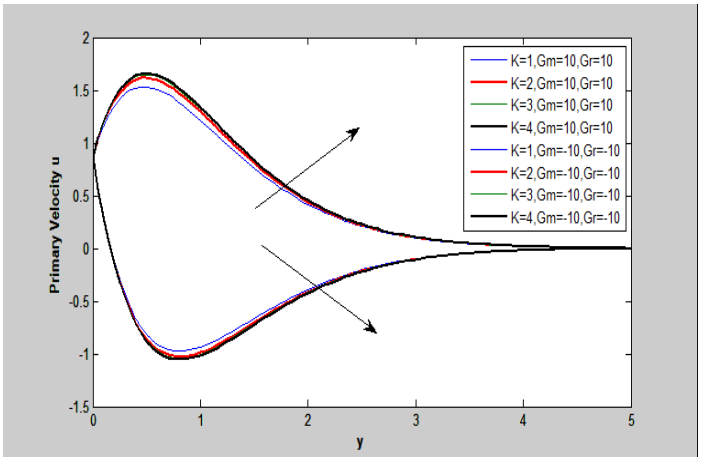

Figure 9: Primary velocity for varying K.

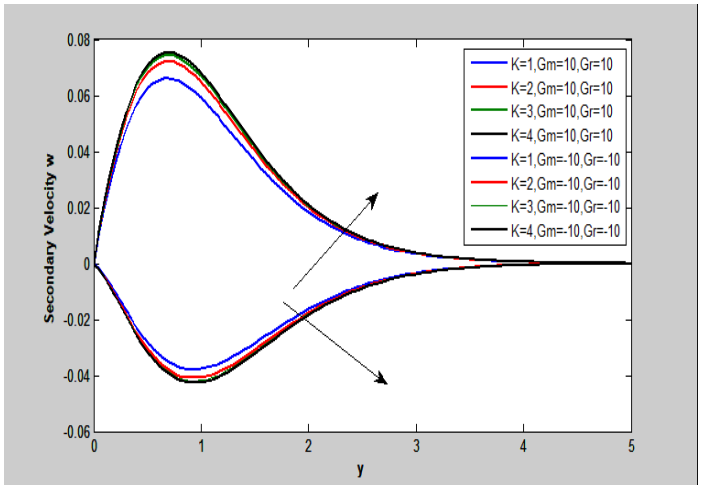

Figure 10: Secondary velocity for varying K.

Secondary velocity is increased due to increase in K. Physically, increase in K tends to decrease the resistance of the porous medium as a result increase the fluid velocity.

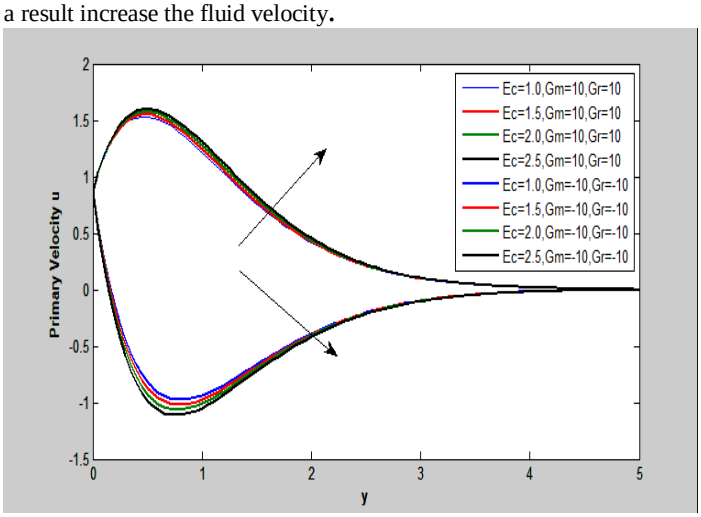

Figure 11: Primary velocity for varying E_c.

From **Figure 11,** E_c expresses the relationship between the kinetic energy in the flow and the boundary layer enthalpy difference. It embodies the conversion of kinetic energy into internal energy by work done against the viscous fluid stresses. It is an important parameter for describing real working fluids in MHD energy generators and materials processing where dissipation effects are not trivial. Positive E_c corresponds to cooling of the wall (plate) and therefore a transfer of heat from the plate to the micropolar fluid. Convection is enhanced and we observe in consistency with that the fluid is accelerated i.e. linear velocity is increased in the micropolar fluid**.**

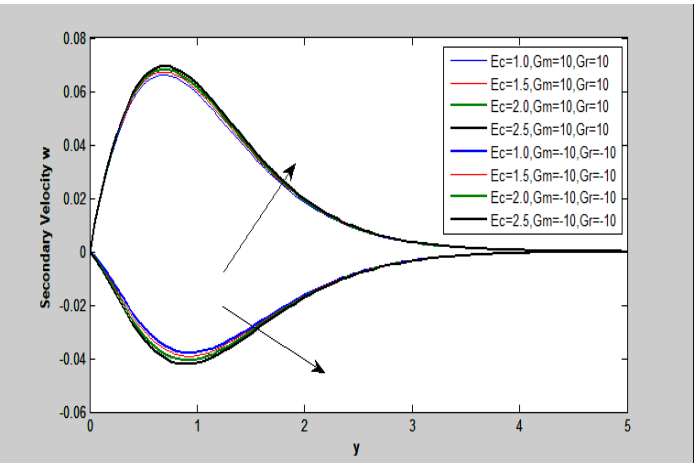

Figure 12: Secondary velocity for varying E_c **.**

E_c expresses the relationship between the kinetic energy in the flow and the boundary layer enthalpy difference. It embodies the conversion of kinetic energy into internal energy by work done against the viscous fluid stresses. It is an important parameter for describing real working fluids in MHD energy generators and materials processing where dissipation effects are not trivial. Positive E_c corresponds to cooling of the wall (plate) and therefore a transfer of heat from the plate to the micropolar fluid. Convection is enhanced and we observe in consistency with that the fluid is accelerated i.e. linear velocity is increased in the micropolar fluid.

Figure 13 shows that the primary fluid velocity is increased with the progression of time. Physically, buoyancy force gradually increases with time as a result fluid velocity enhances.

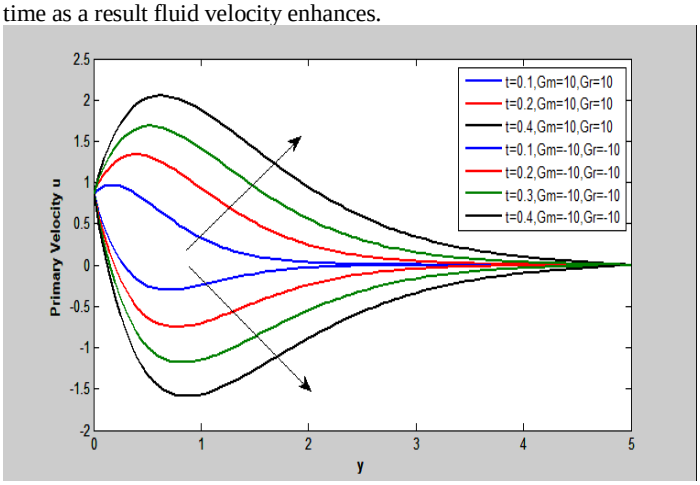

Figure 13: Primary velocity for varying t.

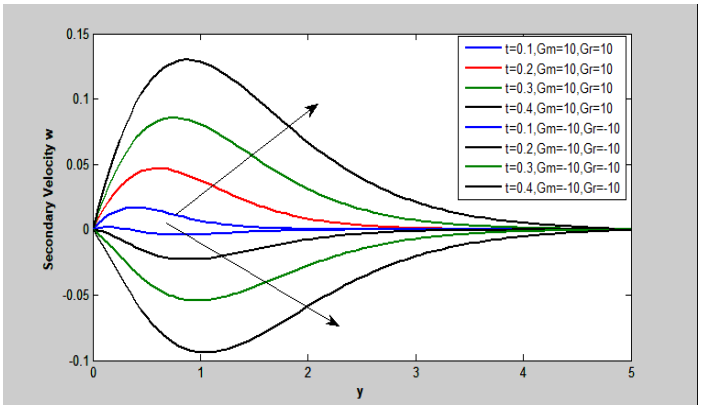

Figure 14: Secondary velocity for varying t.

Figure 14 shows that the secondary fluid velocity is increased with the progression of time. Physically, buoyancy force gradually increases with time as a result fluid velocity enhances in both directions.

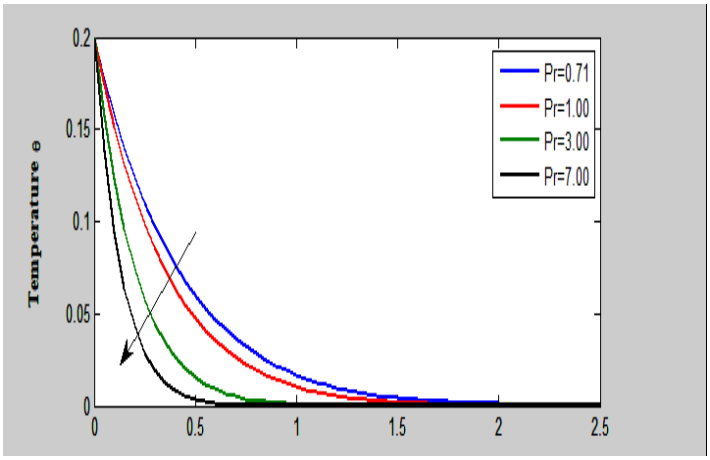

Figure 15: Temperature for varying *Pr*.

It observed that there is a decrease in the temperature and temperature boundary layer as *Pr* increased. This is because the fluid is highly conductive for a small value of *Pr*. Physically, if *Pr* increases, the thermal diffusivity decreases, and this phenomenon leads to the decreasing manner of the energy transfer ability that reduces the thermal boundary layer.

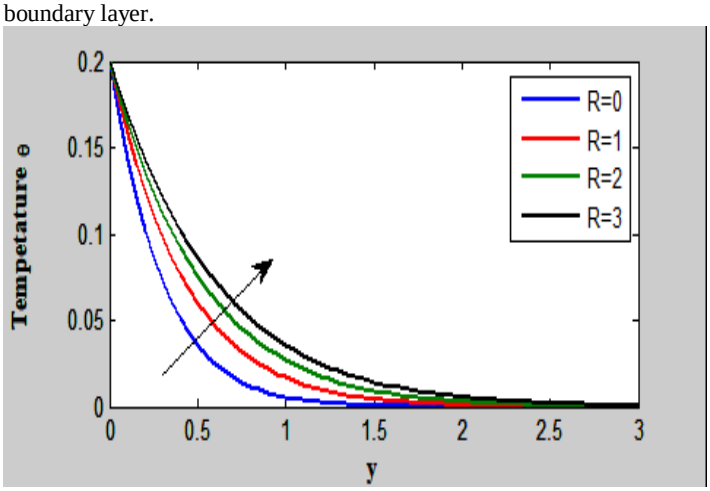

Figure 16: Temperature for varying R.

Global Digital Central
ISSN: 2151-8629

It can be noticed from figure 16 that an increase in R causes improvement of the fluid temperature.

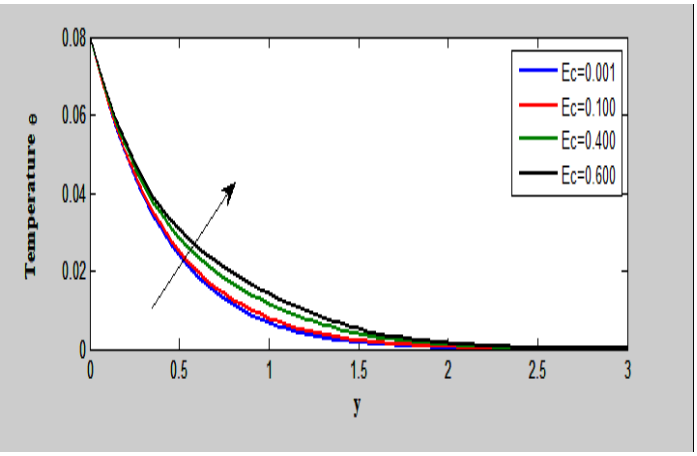

Figure 17: Temperature for varying E_c .

The E_c represents the interrelationship of the flow's kinetic energy and enthalpy. This represents the energy transformation from kinetic to internal in terms of work done against the stress of the viscous fluid. This energy manifests in the form of heat during dissipation. Consequently, the dissipative heat triggers an increase in temperature.

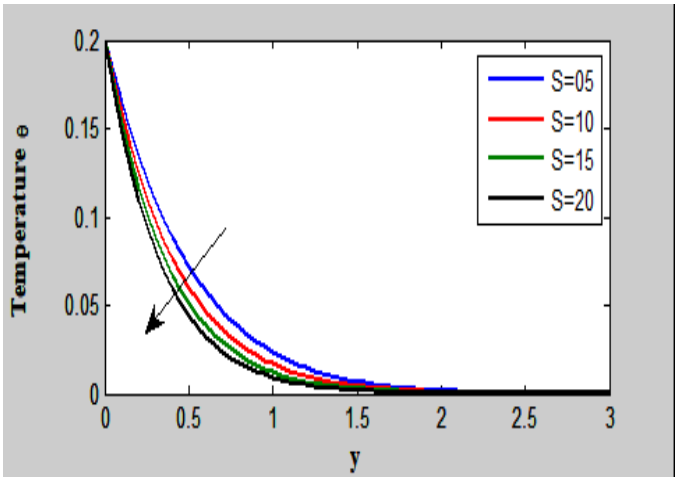

Figure 18: Temperature for varying S .

Figure elucidates that the fluid temperature θ decreases with increasing values of S . When S exists, thermal boundary layer is always starting to be thickened as result fluid temperature depreciate in the boundary layer. The temperature profile follows a trend that is quite similar to the one described in Sharma et al. (2022).

Figure 19 shows that the fluid temperature θ increase with the progression of time t.
It is seen from **figure 20**that the increasing values of *Sc* leads to fall in the concentration distribution. Physically, increase of Sc means decrease of molecular diffusivity D, this results in a decrease of concentration boundary layer. Hence, the concentration of the species is higher for small values of *Sc* and lowers for large values of *Sc*.

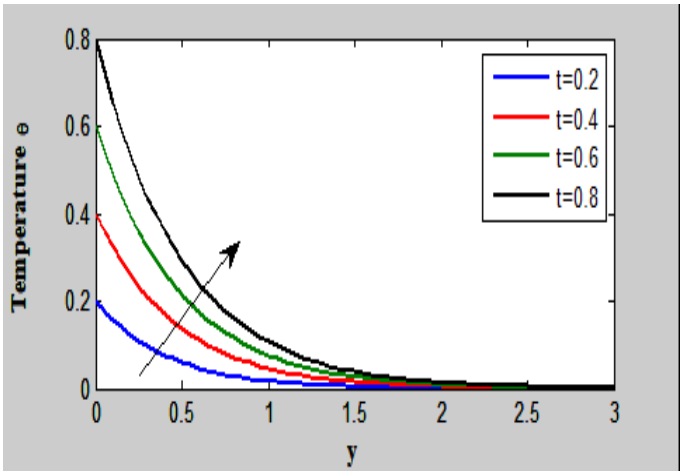

Figure 19: Temperature for varying t.

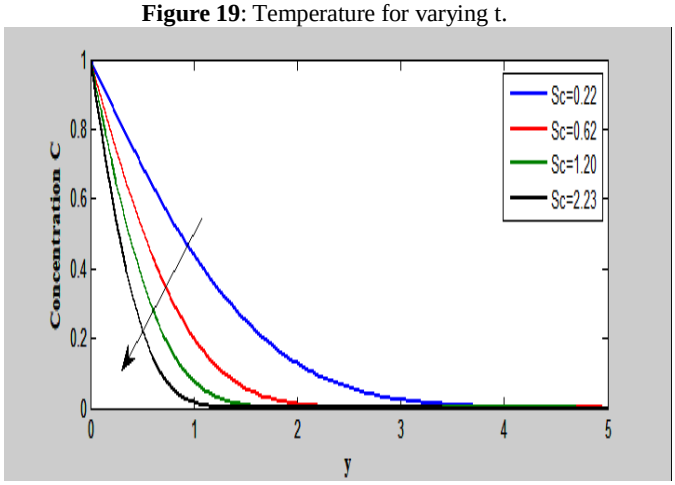

Figure 20: Concentration distribution for varying *Sc*.

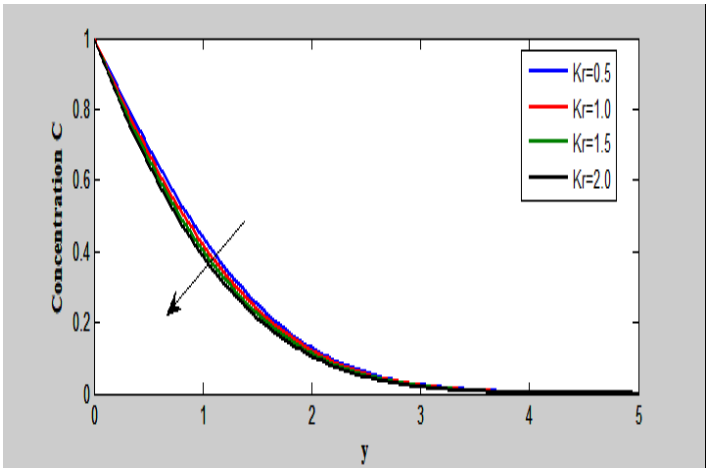

Figure 21: Concentration distribution for varying K_r .

Figure 21 shows a destructive type of chemical reaction because the concentration decreases for increasing K_r which indicates that the diffusion rates can be tremendously changed by K_r .

Global Digital Central
ISSN: 2151-8629

This is due to the fact that an increase in K_r causes the concentration at the boundary layer to become thinner, which decreases the concentration of the diffusing species. This decrease in the concentration of the diffusing species diminishes the mass diffusion

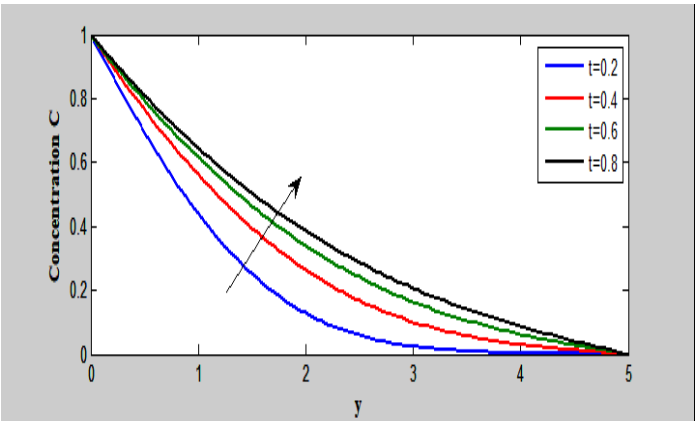

Figure 22: Concentration distribution for varying t.
Concentration increases with progression of time t. Initially, species concentration takes the value 1 and afterward for large values of y it tends to zero with increase of t.

5. CONCLUSIONS

In this paper, the unsteady MHD mixed convective radiating and chemically reacting fluid flow past an impulsively started oscillating vertical plate with Hall current, viscous dissipation, heat source is provided, which is embedded in porous medium. The Galerkin finite element method has been applied to solve the dimensionless governing equations of the flow. It has been found that thermal and mass buoyancy force, Hall parameter, radiation parameter and time tends to accelerate both u and w whereas an increase in Prandtl number, Schmidt number, and chemical reaction rate tends to decelerate both u and w. Increase in the magnetic parameter depreciate u and reverse trend is noticed on w. These parameters have similar effect on both primary and secondary skin frictions.

The fluid temperature enhanced with increment in radiation parameter and time whereas reverse trend is noticed when Prandtl number is increased and opposite effect is noticed on the Nusselt number.

The fluid concentration decline with increment in Schmidt number and chemical reaction rate whereas opposite trend is observed with progression of time and opposite effect is noticed on the Sherwood number. The value of the local skin-friction coefficient increases with increase in porous parameter.

It is expected that the current study of the physics of flow over a vertical surface will serve as the foundation for many scientific and engineering applications involving the flow of electrically conducting fluids. The findings could be valuable in determining the flow of oil, gas, and water through an oil or gas field reservoir, as well as subsurface water migration and filtering and purification procedures. The results of this problem can be helpful in various devices subject to significant variations in gravitational force, its application on heat exchanger designs, wire and glass fiber drawing, and its application in nuclear engineering in connection with reactor cooling.

ACKNOWLEDGEMENTS

The investigators remain profusely grateful to Koneru Lakshmaiah Education Foundation, Vijayawada for extending support and assistance with required permissions during this research study at the Department of Mathematics and to Rise Krishna Sai Prakasam Group of Institutions, Ongole., for according necessary permissions and extending facilities for the work.

Nomenclature

u'	Primary velocity component in x' - direction ($m\ s^{-1}$)
u	Non-dimensional primary velocity ($m\ s^{-1}$)
w'	Secondary velocity component in z' - direction ($m\ s^{-1}$)
w	Non-dimensional secondary velocity ($m\ s^{-1}$)
B_0	uniform magnetic field(Tesla)
ϕ	dimensionless concentration (K)
C'	species concentration
ω'	oscillation frequency
ω	non-dimensional oscillation frequency
C'_w	wall concentration
C'_∞	Concentration of the fluid far away from the plate ($Kg\ \ m^{-3}$)
G_c	mass Grashof's number
G_r	thermal Grashof's number
g	Acceleration of gravity ($m\ s^{-2}$)
q_r	coefficient of Radiative heat transfer
Re	Reynolds number
P_r	Prandtl number
M	magnetic parameter
m	Hall current
T'	near the plate temperature of the fluid
T'_w	plate temperature
T'_∞	temperature of the fluid far away from the plate ($Kg\ \ m^{-3}$)
t	dimensionless time
v	kinematic viscosity ($m^2\ s^{-1}$)
μ	viscosity coefficient
K_r	chemical reaction parameter
D	mass diffusivity ($m\ s^{-2}$)
C_p	Specific heat at constant
ρ	density ($Kg\ \ m^{-3}$)
Ec	Ecerkt Number
S	Heat Source
S_c	Schmidt number
Sh	Sherwood number
Nu	Nusselt number ($J\ Kg^{-1}K$)
τ_x	Primary Skin Friction
τ_z	Secondary Skin Friction
y'	Co-ordinate axis normal to the plate (m)
y	Dimensionless displacement (m)
x'	Coordinate axis along the plate (m)
μ_0	Magnetic Permeability ($N.A^{-2}$)

Greek Symbols:

k	Thermal conductivity of the fluid ($Wm^{-1}K^{-1}$)
θ	Non-dimensional fluid temperature (K)
β	Volumetric coefficient of thermal expansion (K^{-1})

β^* Volumetric Coefficient of thermal expansion with concentration $(m^{-3}\ Kg)$

σ Electric conductivity of the fluid $(s\ m^{-1})$

Subscripts:

∞ Free stream conditions

p Plate

w conditions on the wall

REFERENCES:

Sharma B. K. and Chaudhary R. C., 2008."Hydromagnetic unsteady mixed convection and mass transfer fl ow past a vertical porous plate immersed in a porous medium with Hall effect", *Eng. Trans*.., 56, No. 1, 3–23.

Kishore P.M., Rajesh V., Vijaya kumar Verma S. 2012. "The effects of thermal radiation and viscous dissipation on MHD heat and mass diffusion flow past an oscillating vertical plate embedded in a porous medium with variable surface conditions". *Theoret. Appl. Mech*., 39(2), 99–125.
http://dx.doi.org/10.2298/TAM1202099K

Jithender Reddy G., Srinivasa Raju R. and Siva Reddy Sheri. 2014. "Finite element analysis of soret and radiation effects on transient free convection from an impulsively started infinite vertical plate with heat absorption". *International Journal of Mathematical Archive*, 5(4), 211-220.

Ramana Reddy G.V., Subrahmanyam S.V. Satish Kumar D. 2014. "Soret Effect on MHD Mixed Convection Oscillatory Flow over a Vertical Surface in a Porous Medium with Chemical Reaction and Thermal Radiation". *Ultra Scientist* , 26(1)B, 49-60

Jithender Reddy G., Srinivasa Raju R. ,Manideep P., Anand Rao J. 2016. "Thermal diffusion and diffusion thermo effects on unsteady MHD fluid flow past a moving vertical plate embedded in porous medium in the presence of Hall current and rotating system". *Transactions of A. Razmadze Mathematical Institute* 170, 243–265.
http://dx.doi.org/10.1016/j.trmi.2016.07.001

Srinivasa Raju R., 2017. "Transfer Effects on an Unsteady MHD Mixed Convective Flow Past a Vertical Plate with Chemical Reaction". *Engng.Trans* 65(2), 221–249.
https://et.ippt.gov.pl/index.php/et/article/view/148

Venkateswara Raju K., ParandhamaA. , Raju M.C. , Ramesh Babu K. 2018. "Unsteady MHD free convection jeffery fluid flow of radiating and reacting past a vertical porous plate in slip-flow regime with heat source". *Frontiers in Heat and Mass Transfer (FHMT)*, 10(25).
http://dx.doi.org/10.5098/hmt.10.25

Sitamahalakshmi V., KrishnaSree T. VenkataRamana Reddy G. 2019. "Chemical Reaction and Radiation Effects on MHD Free Convection Flow past an Exponentially Accelerated Vertical Porous Plate". *International journal of basic and applied research*, 9(5).

Prabhakar Reddy B., Muthucumaraswamy R. 2019. "Effects of thermal radiation on MHD chemically reactive flow past an oscillating vertical porous plate with variable surface conditions and viscous dissipation". *i-manager's Journal on Future Engineering & Technology*, 15(2).
https://doi.org/10.26634/jfet.15.2.15020

Shankar Goud B. Srihari K. ,Ramana Murthy M V. 2020. "FDM and FEM correlative approach on unsteady heat and mass transfer flow through a porous medium". *Journal of Xidian University*,14(4), 237.
https://doi.org/10.37896/jxu14.4/237

Saddam Atteyia Mohammad 2020. "Effects of variable viscosity on heat and mass transfer by MHD mixed convection flow along a vertical cylinder embedded in a non-darcy porous medium". *Frontiers in Heat and Mass Transfer (FHMT)*, 14(7).
http://dx.doi.org/10.5098/hmt.14.7

Anil Kumar M., Dharmendar Reddy Y., Srinivasarao V., Shankar Goud B.. 2020. "Thermal radiation impact on MHD heat transfer natural convective nano fluid flow over an impulsively started vertical plate".
https://doi.org/10.1016/j.csite.2020.100826.

Anilkumar M., Dharmendar Reddy Y., Shankar Goud B., Srinivasarao V. 2021. "Effects of soret, dufour, Hall current and rotation on MHD natural convective heat and mass transfer flow past an accelerated vertical plate through a porous medium".
https://doi.org/10.1016/j.ijft.2020.100061

Matao P., Prabhakar Reddy B., Sunzu J., Makinde D.,2020. "Finite element numerical investigation into unsteady MHD radiating and reacting mixed convection past an impulsively started oscillating plate". *International Journal of Engineering, Science and Technology*, 12(1), 38-53.
https://doi.org/10.4314/ijest.v12i1.4

Cowling, T. C. 1957. "Magneto hydrodynamics", *Wiley Inter Science*, New York.

Magyari, E. and Pantokratoras, A. 2011. "Note on the effect of thermal radiation in the linearized Rosseland approximation on the heat transfer characteristics of various boundary layer flows", *International Communications in Heat and Mass Transfer*, 38, 554-556.

Zienkiewiez, O. C. 1971. "The Finite Element Method in Engineering Sciences - 2nd Edition "., McGraw-Hill, New York.

Reddy, J. N. 1985. "An introduction to the finite element method", McGraw-Hill, New York

Bathe, K. J. 1996. "Finite element procedures", Prentice-Hall, New Jersey.

Rajput, U. S. and Kanaujia, N. 2016. "MHD flow past a vertical plate with variable temperature and mass diffusion in the presence of Hall current", *International Journal of Applied Sciences and Engineering*, 14(2), 115.

Sharma BK, Khanduri U, Mishra N .K, Chamkha AJ. 2022. "Analysis of Arrhenius activation energy on magnetohydrodynamic gyrotactic microorganism flow through porous medium over an inclined stretching sheet with thermophoresis and Brownian motion". *Proceedings of the Institution of Mechanical Engineer*.
doi:10.1177/09544089221128768

Sharma B. K, Rishu Gandhi, Nidhish K Mishra and Qasem M. Al-Mdallal. 2022. "Entropy generation minimization of higher-order endothermic/exothermic chemical reaction with activation energy on MHD mixed convective flow over a stretching surface". *Scientific Reports*, 12(1).
https://doi.org/10.1007/978-3-030-99792-2_38.

Global Digital Central
ISSN: 2151-8629

Madhu Sharma, Bhupendra K. Sharma and Bhavya Tripathi. 2022. "Radiation effect on MHD copper suspended nanofluid flow through a stenosed artery with temperature-dependent viscosity". *International*

journal of nonlinear analysis and Applications. 13(2), 2573-2584 https://dx.doi.org/10.22075/ijnaa.2021.22438.2362.

SharmaB.K. and GandhiRishu ., 2022."Combined effects of Joule heating and non-uniform heat source/sink on unsteady MHD mixed convective flow over a vertical stretching surface embedded in a Darcy-Forchheimer porous medium". *Propulsion and Power Reaseach*. 11(2), 276-292
https://doi.org/10.1016/j.jppr.2022.06.001

.

.